Smart antennas based on graphene

Martino Aldrigo,[1] Mircea Dragoman,[1,a)] and Daniela Dragoman[2]
[1]*National Institute for Research and Development in Microtechnology (IMT), P.O. Box 38-160, 023573 Bucharest, Romania*
[2]*Physics Faculty, University of Bucharest, P.O. Box MG-11, 077125 Bucharest, Romania*

(Received 28 July 2014; accepted 3 September 2014; published online 15 September 2014)

We report two configurations of smart graphene antennas, in which either the radiation pattern of the antenna or the backscattering of the periodic metallic arrays is controlled by DC biases that induce metal-insulator reversible transitions of graphene monolayers. Such a transition from a high surface resistance (no bias) to a low surface resistance state (finite bias voltage) causes the radiation pattern of metallic antennas backed with graphene to change dramatically, from omnidirectional to broadside. Moreover, reflectarrays enhance the backscattered field due to the same metal-dielectric transition. © *2014 AIP Publishing LLC*. [http://dx.doi.org/10.1063/1.4895739]

I. INTRODUCTION

The electromagnetic properties of graphene are intensively studied today at microwaves, terahertz (THz), and optical frequencies. In particular, the microwave and millimeter waves propagation in graphene integrated in coplanar waveguides are known up to 110 GHz.[1,2] Graphene as high impedance surface was recently investigated[3] and showed to enhance the gain of various antennas in large bandwidths by suppressing surface waves, which cause multipath interference and backward radiation. Although graphene antennas are studied in microwave and THz domains,[4,5] the most developed area of high-frequency graphene applications is microwave graphene transistors (see Ref. 6 for a recent review). The first integrated graphene receiver at 4.8 GHz has been recently reported,[7] while THz receivers up to 10 THz (Ref. 8) or even 28 THz (Ref. 9) could be fabricated using graphene ballistic rectifiers.

So graphene devices are able to work in a huge bandwidth from RF up to tens of THz. In this context, graphene antennas deserve the same attention as transmission/receiver (T/R) circuits, since a T/R cannot be considered fully integrated without a small and possibly smart antenna integrated with the rest of the circuitry. Tunable optical antennas based on graphene are already fabricated and measured in mid-infrared[10] or visible.[11] Microwave graphene antennas are more problematic since the losses are much higher than in THz or optical domains, especially due to the high conductivity of unbiased graphene, which generates a large imaginary permittivity and in consequence relative high losses, of about −10 to −15 dB (see Refs. 1 and 2). To avoid these losses, which could induce relatively low radiation efficiencies, we avoid using graphene as an antenna, but use it instead as a tunable reflector. Biased graphene backing the substrate of small metallic antennas confers tunability, reconfigurability, and better directivity to antennas, via DC-controlled metal-insulator transition. In brief, biased graphene makes a metallic antenna smart. The paper is divided in two parts. In the first part, we analyze an electrical small dipole on high resistivity (HR) Si backed graphene, while in the second part we analyze a reflectarray with metallic patches backed by graphene and show that the reflection properties of this array change due to tunable reflections.

II. SMART SMALL METALLIC DIPOLES ON HIGH ELECTRICAL PERMITTIVITY DIELECTRICS BACKED BY GRAPHENE

The configuration of this smart antenna, depicted in Fig. 1(a), consists of a metallic dipole deposited on HR Si, which is used further as substrate to grow SiO_2 and graphene (see Fig. 1(b)). The graphene on its turn is acting as a reflector for the metallic dipole.

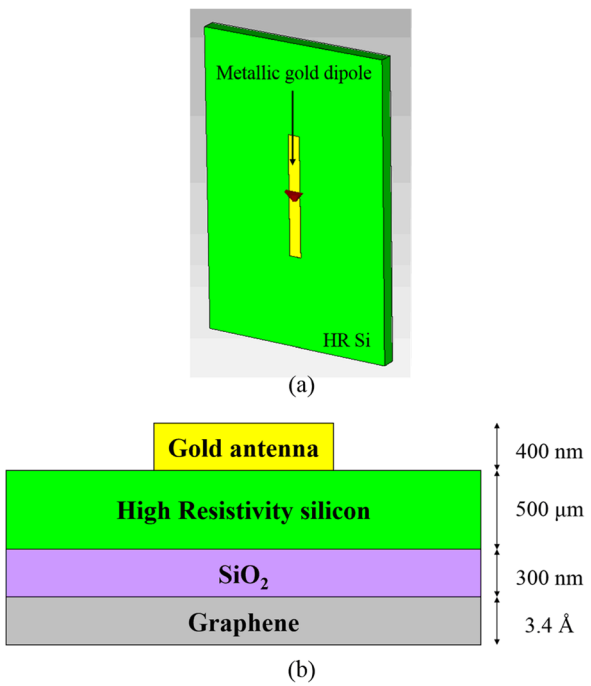

FIG. 1. (a) Schematic representation of the dipole on HR Si, and (b) cross-section of the smart graphene-based metallic dipole antenna.

a)Author to whom correspondence should be addressed. Electronic mail: mircea.dragoman@imt.ro.

The real part of the intraband conductivity in graphene prevails over the imaginary part, which is very small up to few THz. We have, thus

$$\sigma(\omega) = -ie^2 k_B T/\pi\hbar^2(\omega - i2\Gamma)[(\mu/k_B T) + 2\ln(\exp(-\mu/k_B T) + 1)], \quad (1)$$

where T is the temperature, $\Gamma = 1/\tau$ is an energy-independent scattering rate with $\tau = 0.1$ ps, and $\mu \cong e\alpha V_b$ is the chemical potential with α a constant depending on the device geometry and V_b the bias voltage. The surface impedance is then

$$Z_S(V_b) = 1/\sigma(\omega) = R_s(V_b) + jX_s(V_b). \quad (2)$$

$Z_S(V_b)$ depends strongly on the bias voltage, such that both R_s and X_s can be tuned between 50 Ω–2 kΩ and 0.2–3 Ω, respectively, by applied voltages. So, from an electromagnetic point of view, graphene acts as a good metallic-like reflector when it is biased and as a lossy dielectric when unbiased.

The dipole in Fig. 1(a), with dimensions: length of 4.18 mm, width of 0.42 mm, and distance between the metallic dipole and the graphene reflector of $\lambda_0/15$, is small compared to the wavelength $\lambda_0 = 3$ cm, which corresponds to a frequency of 10 GHz. In consequence, the electrical matching problem is difficult and low radiation efficiency is expected.

In order to find the resonant frequencies of the dipole in the case when the graphene is biased or not, it is needed first to know the input impedance of the antenna. All simulations in this paper are performed with the help of CST software. The frequency dependence of the input impedance is represented in Fig. 2. From this figure it follows that the resonance frequency, which corresponds to $\mathrm{Im}\, Z_{in} = 0$, shifts from 14.6 GHz when graphene has $R_S = 5$ kΩ to 10.8 GHz when $R_S = 5$ Ω. So biasing of the graphene reflector induces an important shift of the resonance frequency, with a maximum bandwidth of 4 GHz.

From the radiation patterns corresponding to these two extreme values of R_S, displayed in Fig. 3, it can be seen that the electromagnetic field behaves very differently in the two situations. When $R_S = 5$ kΩ and graphene is acting as a lossy dielectric, the electromagnetic field is uniformly distributed

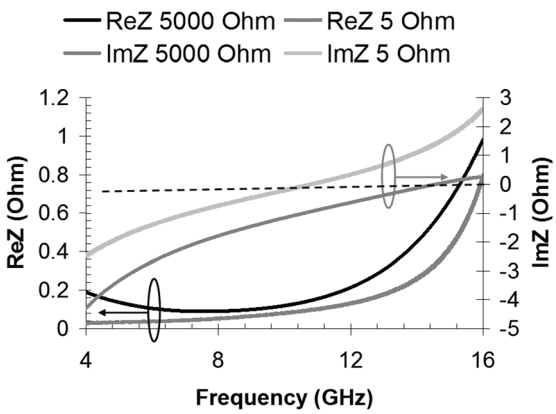

FIG. 2. The input impedance of the antenna.

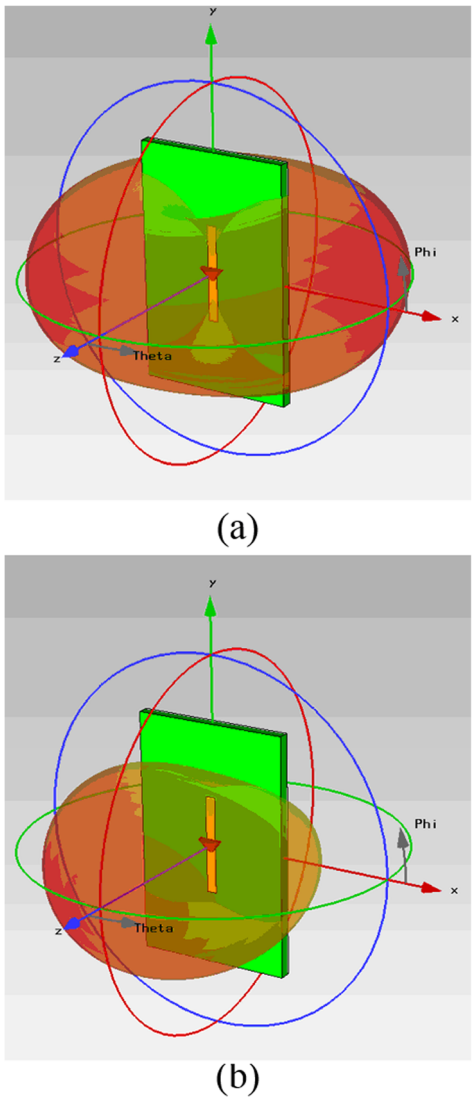

FIG. 3. The radiation pattern of the antenna (a) at 14.6 GHz for $R_s = 5$ kΩ and (b) at 10.8 GHz for $R_s = 5$ Ω.

in all directions, and we have an omnidirectional radiation pattern, typical for dipole antennas, as is the studied dipole. This means that the graphene plays no role in the dipole radiation, and the antenna directivity is low, of 2.2 dBi. However, when $R_S = 5$ Ω, the electromagnetic field is confined, the radiation pattern becomes broadside, and the directivity is doubled, reaching a value of 4.6 dBi. In this case, graphene acts as a reflector, enhancing the directivity of the antenna radiation. Therefore, the radiation pattern of the antenna is reconfigurable, i.e., is tunable with the applied DC bias, and the antenna becomes "smart." This property could have huge applications, because the antenna can be used to transmit in all directions if unbiased, while, when biased, the same antenna can be used as a receiver, to get more power at a certain direction. Many other applications, including an adaptive receiver, can be envisaged with such a reconfigurable antenna.

Moreover, the antenna can be easily matched with LC circuits, the resulting simulations of the reflection coefficients being represented in Fig. 4. These simulations show good matching at the two frequencies, 10.8 GHz and

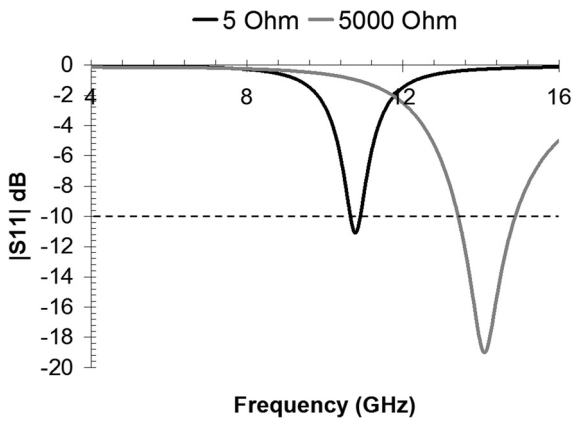

FIG. 4. The reflection coefficient S11.

14.6 GHz, corresponding to the two values of surface resistance of graphene.

III. REFLECTARRAYS

A reflectarray is a planar reflecting surface formed from elements with controllable impedance. When an incoming wave is directed towards this reflectarray, a prescribed radiation pattern is obtained.

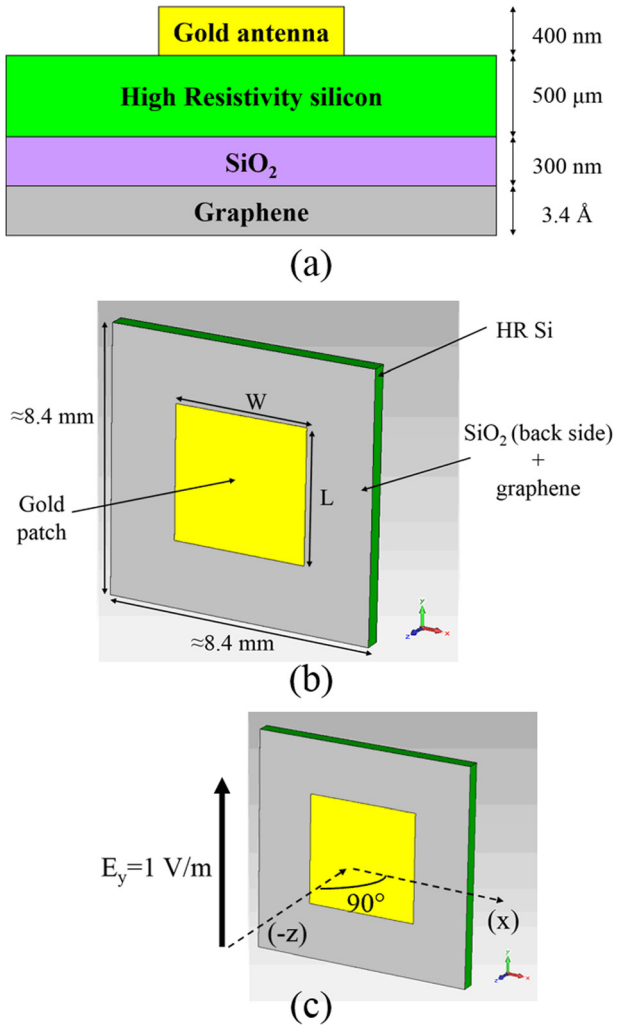

FIG. 5. (a) The cross-section of the reflectarray element, (b) top view of the radiating element, and (c) geometry of plane wave excitation.

The configuration of the reflectarray element studied in this paper is represented in Figs. 5(a)–5(c). We have calculated first the reflection coefficient of the unit cell, depicted in Fig. 6, when the plane wave is incident at 45° with respect to the element of the reflectarray. We have computed the amplitude and the phase of the reflection coefficient in three situations: biased graphene, unbiased graphene, and only gold metal, in the absence of graphene. We found that the reflection coefficient of the reflecting element in the case of biased graphene is similar to that of the reflecting element made of gold with no graphene, except that no detrimental peaks in S11 phase jumps are observed for biased graphene. The peaks in reflection and the associated phase jumps are due to surface waves formed on gold and suppressed by a high conductive surface like graphene. The reflection for the unbiased case is lower than for the other cases, and, again, presents no resonances.

The geometry of the reflectarray composed of 10×10 reflection elements with the properties described above is illustrated in Fig. 7. Its dimensions make allow its fabrication on a 4×4 in. of chemical vapor deposition (CVD) grown graphene wafer. In Fig. 8, we have represented the backscattered electric field of the reflectarray at normal incidence of the plane wave. This field presents a maximum at $\theta = 0°$ for both cases of unbiased and biased graphene, but with an

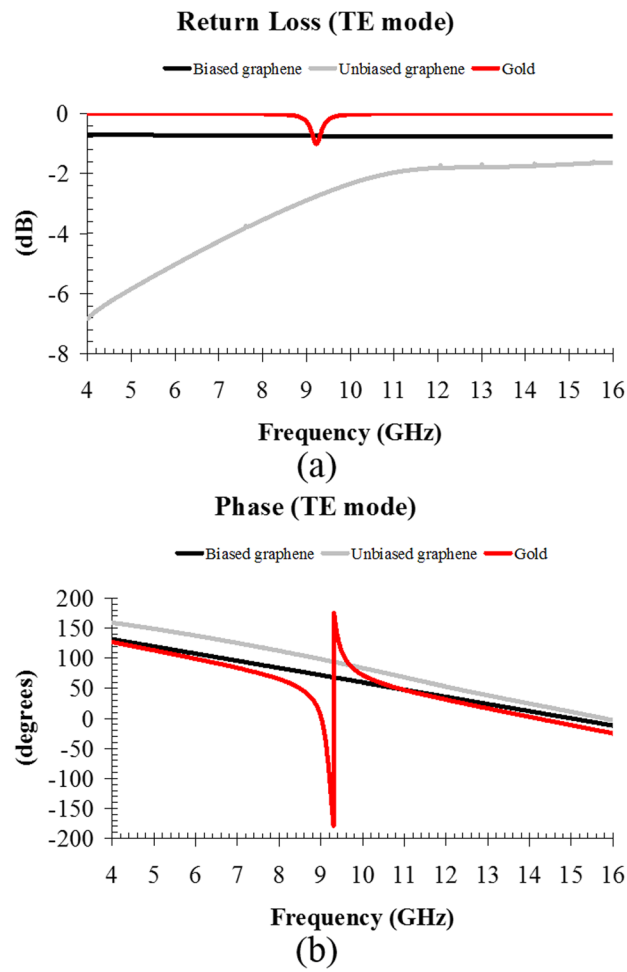

FIG. 6. The (a) amplitude and (b) phase of the reflected field of the reflection element represented in Fig. 5.

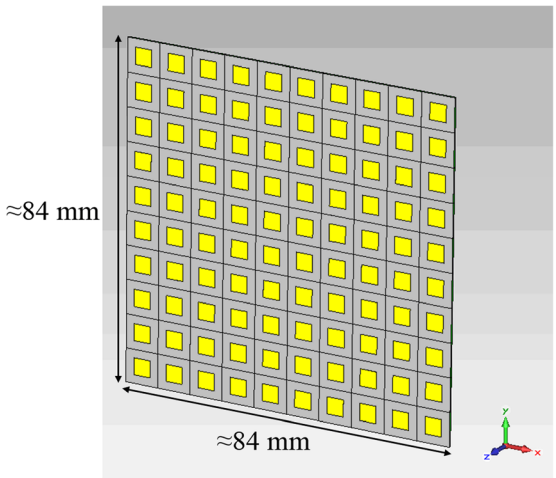

FIG. 7. Schematic representation of the 10 × 10 reflectarray.

important difference: when biasing the graphene, the maximum value of the electric field is −13.75 dB V/m, whereas the maximum value for unbiased graphene is about −20 dB. The difference, of $\Delta E \approx 6.25$ dB, indicates that the backscattered power with biased graphene is 4 times greater than for unbiased graphene in the direction of reflection. This difference is even bigger if we consider the side lobes, where it reaches a value of almost 19 dB.

IV. DISCUSSION

Surface resistance metal–insulator transition is the key physical principle of the above smart antennas. The reversible transition between a high resistance state to a low resistance state and vice versa is achieved by applying a DC voltage. So the DC voltage values and bias circuit architecture are very important for smart graphene antennas. We compute in Fig. 9 the real and imaginary parts of the surface resistance $Z_s = R_s + jX_s$ at 10 GH as a function of the bias voltage V_b both computed in logarithmic scale with values in the range of 1 mV–50 V, for scaling purposes. The two curves were obtained by applying the Kubo formula with $T = 300$ K and $\tau \approx 0.4$ ps. The range for R_s is about 5 Ω–5 kΩ (three orders of magnitude), while the range for X_s is about 0.01 Ω–7 Ω (two orders of magnitude). As already stated, the imaginary part of the surface impedance is practically

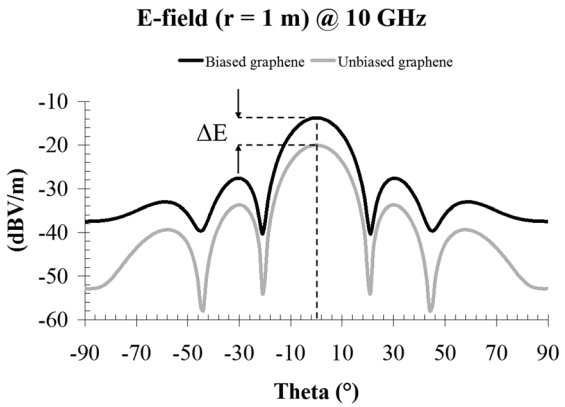

FIG. 8. The backscattered field of the reflectarray.

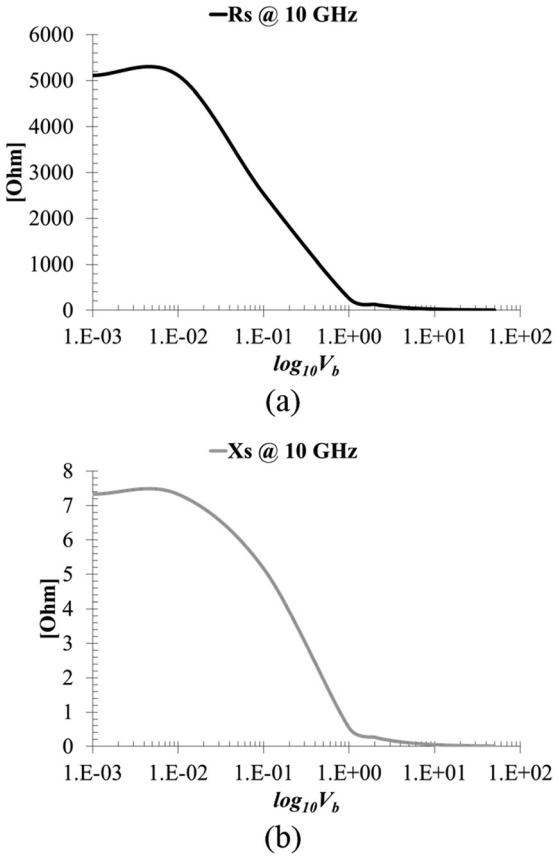

FIG. 9. The logarithm of real part and imaginary part of the graphene surface resistance versus logarithm of the applied voltage.

negligible with respect to the real one, hence graphene can be considered in reason a tunable resistive surface. We see that at only 1 V, the surface resistance decreases below 150 Ω. To reach lower surface resistances, it is necessary to increase the voltage up to 20–30 V. These high DC voltages are not a problem for the graphene because in any bias configuration, i.e., back-gate or top gate, the bias is not applied directly on graphene, graphene being protected in all bias configurations by an insulator, i.e., an oxide such as SiO_2 or HfO_2 deposited using various methods over it and having a thickness in the range of 20–200 nm depending on the oxide material and the quality of the deposition. Further, on the oxide, a metallic electrode playing the role of the gate is further deposited.

However, the back gate configuration which is widespread in graphene devices cannot be applied for microwave graphene device working beyond 5–6 GHz because the doped Si substrate which is the widespread back-gate material shows high electromagnetic losses in microwaves.

However, our particular configuration allows a different configuration. We can have a top-gate configuration on the graphene placed at the bottom of the smart antennas and thus the DC bias for metal-insulator transistor will be only few volts. We note that such top-gate-bias cannot be used for any other graphene antenna geometries found in the literature and cited in Refs. 4 and 5 and the references therein. The reason is that the graphene itself is forming the antenna and thus the graphene antenna cannot be covered with an oxide and further a metallic electrode because will no longer

radiate. In our case, the graphene is placed at the bottom of the antenna and its role is to change the reflection conditions of the antenna and is not an electromagnetic radiator. So, practically, we will deposit a thin oxide layer over graphene and further a gate metal deposition over it. Although the gate is placed at the backside of the antenna, it is a top-gate-like configuration for graphene and no doped Si is used. This solution is extended in the case of the reflect array at the wafer level by implementing a top gate bias configuration for all antenna having a cross-bar geometry such that all the antennas to be fed at the same voltage. Only in this way, the reflectarray is tunable.

Could we extend our findings of the smart antenna on graphene using other 2D materials? The answer is not straightforward. The 2D materials like metallic chalcogenides are semiconductors and they cannot still be easily produced at the wafer scale like graphene. Other known 2D materials are semiconductors or isolators and such metal–dielectric transitions are studied nowadays using first principle calculations. The presence of such transitions by applying a DC signal was recently experimentally evidenced.[12] The recent experiment about the metal-insulator transition in a MoS_2 monolayer has shown that the charge density can be tuned with more than $3.6 \times 10^{13}\,cm^{-2}$ (Ref. 12) via a top-gate voltage similar to graphene, where even a tuning of $10^{16}\,cm^{-2}$ can be obtained via solid electrolytes.[13] Adding to these facts that recently it was demonstrated that high quality MoS_2 monolayers can be grown via CVD on various substrates such as silicon oxide, sapphire, or graphite and having an area of few centimeters,[14] we conclude that smart antennas as described above could be fabricated and tested on MoS_2 monolayers.

V. CONCLUSIONS

We have analyzed two graphene-based antennas in which the radiation pattern of the antenna or the backscattering of a 10×10 reflectarray can be controlled by metal-insulator reversible transitions of biased graphene monolayers. We have found that the radiation patterns of metallic antennas backed with graphene are reconfigurable, from omnidirectional to broadside, by changing the DC voltage. On the other hand, reflectarrays enhance the power of the backscattered field due to the same metal-dielectric transition. These examples show that the physical properties of graphene confer to the electromagnetic structures analyzed in this paper new electromagnetic properties, such that this radiating devices based on graphene can be termed as "smart." In particular, a smart phone, which has no antennas of the type described here, could become even smarter in the future, if it would integrate such devices able to adapt at various transmission or receiving working modes of the electromagnetic field.

ACKNOWLEDGMENTS

We thank the European Commission for the financial support via the FP 7 NANO RF (Grant Agreement No. 318352).

[1]M. Dragoman, D. Neculoiu, A. Cismaru, A. A. Müller, G. Deligeorgis, G. Konstantinidis, D. Dragoman, and R. Plana, "Coplanar waveguide on graphene in the range 40 MHz–110 GHz," Appl. Phys. Lett. **99**, 033112 (2011).
[2]H. S. Skulason, H. V. Nguyen, A. Guermoune, V. Sridharan, M. Siaj, C. Caloz, and T. Szkopek, "110 GHz measurement of large-area graphene integrated in low-loss microwave structures," Appl. Phys. Lett. **99**, 153504 (2011).
[3]M. Aldrigo, M. Dragoman, A. Costanzo, and D. Dragoman, "Graphene as a high impedance surface for ultra-wideband electromagnetic waves," J. Appl. Phys. **114**, 184308 (2013).
[4]D. Mencarelli, M. Dragoman, L. Pierantoni, T. Rozzi, and F. Coccetti, "Design of a coplanar graphene-based nano-patch antenna for microwave application," in Internal Microwave Symposium, Tampa, Florida, USA (2013).
[5]E. Carrasco and J. Perruisseau-Carrier, "Reflectarray antenna at terahertz using graphene," IEEE Antennas Wireless Propag. Lett. **12**, 253–256 (2013).
[6]Y. Wu, K. A. Jenkins, A. Valdes-Garcia, D. B. Farmer, Y. Zhu, A. A. Bol, C. Dimitrakopoulos, W. Zhu, F. Xia, P. Avouris, and Y.-M. Lin, "State-of-the-art graphene high-frequency electronics," Nano Lett. **12**, 3062–3067 (2012).
[7]S.-J. Han, A. Valdes Garcia, S. Oida, K. A. Jenkins, and W. Haensch, "Graphene radio frequency receiver integrated circuit," Nat. Commun. **5**, 3086 (2014).
[8]M. Dragoman, M. Aldrigo, A. Dinescu, D. Dragoman, and A. Costanzo, "Towards a terahertz direct receiver based on graphene up to 10 THz," J. Appl. Phys. **115**, 044307 (2014).
[9]Z. Zhu, S. Joshi, S. Grover, and G. Moddel, "Graphene geometric diodes for terahertz rectennas," J. Phys. D: Appl. Phys. **46**, 185101 (2013).
[10]Y. Yao, M. A. Kats, R. Shankar, Y. Song, J. Kong, M. Loncar, and F. Capasso, "Wide wavelength tuning of optical antennas on graphene with nanosecond response time," Nano Lett. **14**, 214–218 (2014).
[11]Z. Fang, Z. Liu, Y. Wang, P. M. Ajayan, P. Nordlander, and N. J. Halas, "Graphene-antenna sandwich photodetector," Nano Lett. **12**, 3808–3813 (2012).
[12]B. Radisavljevic and A. Kis, "Mobility engineering and a metal–insulator transition in monolayer MoS_2," Nat. Mater. **12**, 815–820 (2013).
[13]T. Low and P. Avouris, "Graphene plasmonics for terhertz and mid-infrared applications," ACS Nano **8**, 1086–1101 (2014).
[14]Y. Yu, C. Li, Y. Liu, L. Su, Y. Zhang, and L. Cao, "Controlled scalable synthsis of uniform, high quality monolayer and few layer MoS_2 films," Sci. Rep. **3**, 1866 (2013).